

# A Method of Representing the Nonisothermal Effectiveness Factor for Fixed Bed Calculations

J. G. JOUVEN and RUTHERFORD ARIS

Department of Chemical Engineering  
University of Minnesota, Minneapolis, Minnesota 55455

A parametric representation of the effectiveness factor for a first-order, nonisothermal irreversible reaction in a catalyst pellet has been devised that amply covers the realistic range of parameters for the exothermic case. Given the Thiele modulus, Prater temperature, and dimensionless activation energy, the effectiveness factor can be recovered in about 1/1000 sec. (CDC 6600) to an accuracy of better than 5% over most of the range. When heat and mass transfer resistance at the surface is added the time required is about 0.03 sec. This makes fixed bed calculations more than 50 times faster than would otherwise be possible.

When a chemical reaction takes place in a catalyst pellet the interaction of diffusion and reaction is commonly expressed in terms of an effectiveness factor, the ratio of the actual reaction rate to that which would obtain were there no diffusive limitations. This characteristically chemical engineering device appears in the independent, but almost simultaneous, work of Damköhler (10), Thiele (18), and Zeldovich (21) in the late 1930's and early 1940's and is one of the few aspects of the early work that the physicist Jüttner did not anticipate in 1909 (11). This first work treated the isothermal case for several orders of reaction, and it was not until the early 1960's that nonisothermal effectiveness factors were published again, independently and almost simultaneously, by Weiss and Hicks (19), Amundson and Schilson (2), Carberry (6, 7, 9), Metzner and Tinkler (15). From the nonisothermal studies it became evident that for sufficiently exothermic reactions there could be three steady states over a certain range of the Thiele modulus, a discovery that has produced much interesting theoretical work in the last decade.

The effectiveness factor is a functional of the solution of a second-order differential equation with two-point boundary conditions and although with the proper precautions it is a straightforward enough matter to compute, it is sufficiently time-consuming to be out of the question normally to compute it for each particle in a fixed bed calculation. Realizing this, some workers have pointed out that in many cases the particle can be regarded as isothermal with heat transfer resistance concentrated at the surface. This allows the comparatively simple formulae for the isothermal effectiveness factor to be exploited. Liu (12) however has taken a rather different approach and sought to fit the computed results by a simpler empirical expression which can be called up on the computer in a fraction of the time it would take to solve the differential

equation. On the basis of this he was able to do fixed bed calculations taking into account the diffusive effects in the particle. The present paper reports work in which a best-fitting interpolation formula has been used to provide a rapid way of calculating the effectiveness over a much wider range of parameters than Liu was able to take into account and specifically to be able to handle the region where there may be more than one steady state.

## The Range of the Effectiveness Factor and the Parameters on Which it Depends

The first order irreversible reaction will be considered to take place in a spherical particle. The equations governing this model are well-known and need not be derived in detail. They are

$$\frac{d^2x}{d\rho^2} + \frac{2}{\rho} \frac{dx}{d\rho} = \phi^2 x \exp \left\{ \beta \gamma \frac{1-x}{1+\beta(1-x)} \right\} \quad (1)$$

with

$$\frac{dx}{d\rho} = 0 \quad \text{at} \quad \rho = 0 \quad (2)$$

and

$$x = 1 \quad \text{at} \quad \rho = 1 \quad (3)$$

Here

- $x$  = dimensionless concentration of reactant = ratio of concentration at  $r$  to surface concentration  $c_s$
- $\rho$  = dimensionless radial position in the sphere =  $r/R$
- $R$  = radius of spherical particle
- $\phi$  = Thiele modulus =  $R^2 \rho_b S_g k_s / D_e$
- $\rho_b$  = bulk density of particle
- $S_g$  = catalytic area per gram
- $k_s$  = first order rate constant evaluated at surface temperature,  $T_s$
- $D_e$  = effective diffusivity of reactant in particle
- $\beta$  =  $(-\Delta H) D_e c_s / k_e T_s$

J. G. Joven is with Universal Oil Products, Des Plaines, Illinois.

$\Delta H$  = heat of reaction  
 $k_e$  = effective thermal conductivity of the particle  
 $\gamma = E/R_g T_s$   
 $E$  = activation energy of reaction  
 $R_g$  = gas constant

When the solution of this equation is calculated the effectiveness factor is given by

$$\eta = \frac{3}{\phi^2} \left( \frac{dx}{d\phi} \right)_{\phi=1} \quad (4)$$

A typical set of curves, such as given by Weiss and Hicks is shown in Figure 1 for  $\gamma = 40$ ,  $\beta = 0.1, 0.2$ , and  $0.3$ . For the lowest curve there is a unique value of  $\eta$  for each value of  $\phi$ , but for  $\beta = .2$  or  $.3$  there is a range of  $\phi$  over which the curve bends back and there are three values of  $\eta$  for each  $\phi$ . It might be expected that there is a value of  $\beta$  (it is actually about  $0.12$ ) for which the curve has a vertical tangent at its inflection point (shown as a broken curve) which separates curves giving a unique  $\eta$  from those that do not.

A common approximation (15, 16) has been to regard the curves as functions of one parameter instead of two, namely

$$\delta = \beta\gamma \quad (5)$$

The possibility of doing this can be seen from Equation (1) where if  $\beta(1-x) \ll 1$  in the denominator of the argument of the exponential, it can be neglected and leave the field to the only remaining parameter  $\beta\gamma = \delta$ . Carberry (6) has shown that this is not a bad approximation if  $\delta < 6$ , and Liu (12) restricts himself to this range. However, this excises a large part to the range of nonuniqueness which is under consideration here.

A fuller discussion of the realistic range of the parameters  $\beta$  and  $\gamma$  is given elsewhere (14), suffice it to say that attention has been directed to this point by several authors (8, 11, 13) and that the range of the parametric fitting done here is an ample one. Figure 2 shows the exothermic

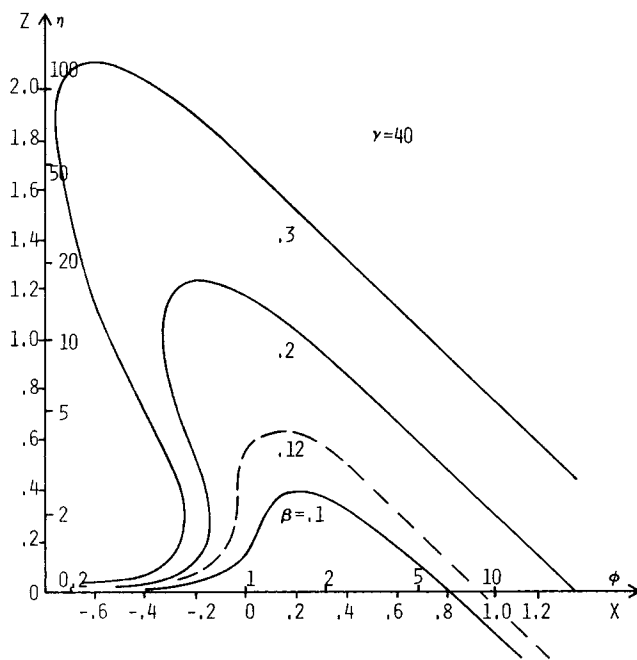


Fig. 1. Effectiveness factor versus Thiele modulus for  $\gamma = 40$ ,  $\beta = 0.1, 0.2, 0.3$ . Broken curve for  $\beta = 0.12$  has a vertical tangent at its inflection point.

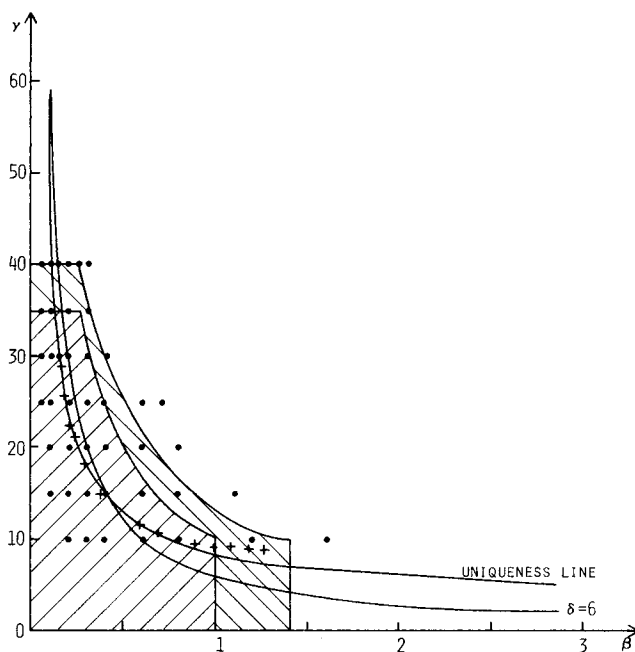


Fig. 2. The exothermic  $\beta, \gamma$ -plane. The hatched areas are covered by the method of this paper, the inner one to better than 5%, the outer with 5 to 10% accuracy. The dots denote  $\beta, \gamma$ -values used in the fittings. The crosses are  $\beta, \gamma$  pairs giving a curve with vertical tangent at inflection and may be compared with the exact uniqueness line. The hyperbola  $\delta = 6$  is also shown.

part of the  $\beta, \gamma$ -plane. The area under the curve  $\delta = 6$  is the region for which Liu claims "reasonable" accuracy. The two shaded regions are those covered by our results in the smaller of which the interpolation formula is accurate to within 5%, whereas only 10% accuracy can be claimed in the larger. The endothermic part of the plane presents no difficulties as Liu points out (12).

#### The Principal of the Method

The entire study will be done in the plane of  $X = \log_{10}\phi$  and  $Z = \log_{10}\eta$ . In very rough form the curves look like the bent line ABPC in Figure 3a in which  $OA = a$ ,  $OB = b$ ,  $OC = c$  and since the slope of PC is  $-1$ ,  $BP = l$  where

$$l^2 = (b-a)^2 + (c-a)^2 \quad (6)$$

The parametric representation of the broken line would be

$$\sigma \leq b, \quad X = \sigma, \quad Z = 0$$

$$b \leq \sigma \leq b+l, \quad X = b + (a-b)(\sigma-b)/l, \quad Z = (c-a)(\sigma-b)/l \quad (7)$$

$$b+l \leq \sigma, \quad X = a + 2^{-1/2}(\sigma-b-l), \quad Z = (c-a) - 2^{-1/2}(\sigma-b-l)$$

The parameter  $\sigma$  is evidently the distance on the "curve" from  $X = 0, Z = 0$ . Obviously this representation is crude and the corners need to be rounded.

Consider the function

$$F(\sigma; a, n) = \{1 + e^{-n(\sigma-a)}\}^{-1} \quad (8)$$

It is a "soft" step function going from 0 to 1 as  $\sigma$  passes from  $a - \infty$ . It is shown in Figure 3b for several values of  $n$  and clearly, the larger  $n$  the sharper the step. The function  $F$  is used to define three new functions whose behavior is shown in parts c, d, and e of Figure 3.

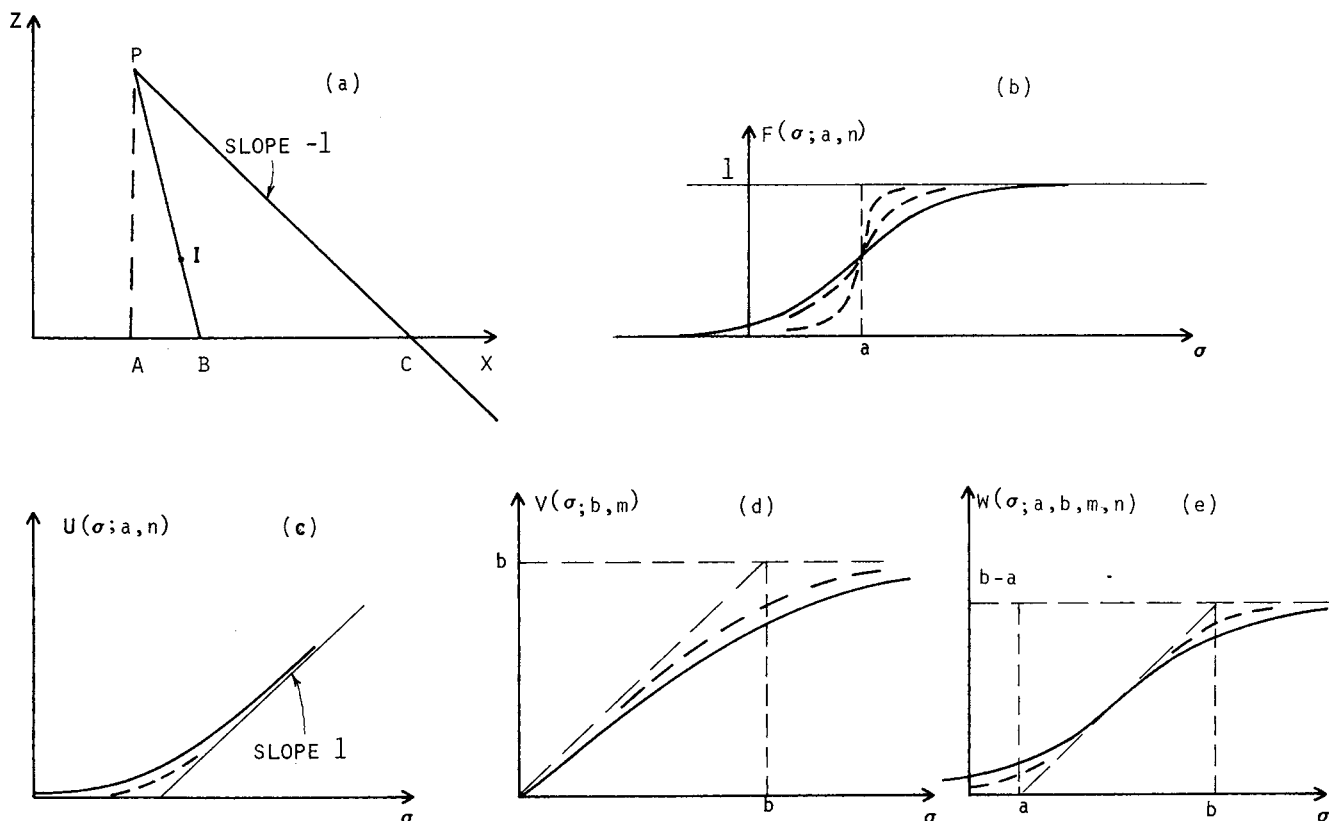


Fig. 3. a. The broken line. b. The function  $F$  for various  $n$ . c.  $U(\sigma; a, n)$ . d.  $V(\sigma; b, m)$ . e.  $W(\sigma; a, b, m, n)$ .

$$U(\sigma; a, n) = \int_{-\infty}^{\sigma} F(\tau; a, n) d\tau = \frac{1}{n} \ln \{e^{n(\sigma-a)} + 1\} \quad (9)$$

$$V(\sigma; b, m) = \sigma - U(\sigma; b, m) \quad (10)$$

and

$$W(\sigma; a, b, m, n) = U(\sigma; a, m) - U(\sigma; b, n) \quad (11)$$

These three functions can be put together to give curves of the form of Figure 1. It may be noted that it will not be necessary to split the range of  $\sigma$  up into segments with different formulae for each and that as  $n \rightarrow \infty$  the bent line form is reached. The combined formula then is

$$X(\sigma) = V(\sigma; b, m) + \{(a-b)/l\}$$

$$W(\sigma; b, b+l, m, n) + 2^{-1/2} U(\sigma; b+l, n) \quad (12)$$

$$Z(\sigma) = \{(c-a)/l\} W(\sigma; b, b+l, m, n) - 2^{-1/2} U(\sigma; b+l, n) \quad (13)$$

The parameter  $\sigma$  is no longer the length along the curve though  $\sigma = b$  and  $\sigma = b+l$  mark the corners in a rough way. There are thus five shape parameters  $a, b, l, m$ , and  $n$  and the challenge is to relate these to the physical parameters  $\beta$  and  $\gamma$  so as to give a good representation.

#### Refinement of the Model

In searching for a best fit the method of Hooke and Jeeves was used; a clear description of this method is given by Wilde (20). The attempt was first made to fit one curve well and then to extend this to a family of curves. The curve chosen was for  $\beta = 0.6$ ,  $\gamma = 20$  on which 36 points were first computed. Let these points be denoted by  $(X_{ci}, Z_{ci})$   $i = 1, 2, \dots, 36$ . Then it might be possible

to choose  $\sigma_i$  for each point by  $X(\sigma_i) = X_{ci}$  and choose  $a, b, m$ , and  $n$  to minimize  $I(a, b, m, n) = \sum_{i=1}^{36} \{Z(\sigma_i) - Z_{ci}\}^2$ . However the  $X$ -coordinate doubles back on itself so that  $\sigma_i$  cannot be uniquely determined. This difficulty was circumvented by defining

$$Y(\sigma) = 2X(\sigma) + Z(\sigma) \quad (14)$$

which has a one-valued inverse and allows  $\sigma_i$  to be determined by

$$Y(\sigma_i) = Y_{ci} = 2X_{ci} + Z_{ci} \quad (15)$$

However, the formula for  $Y(\sigma)$  contains several exponentials and the inverse function is not easy to compute.

After several attempts it became apparent that this model was too crude particularly in forcing the curves to appear more symmetrical than in fact they were. It appeared that the parameters were too interdependent and did not sufficiently correspond to the natural characteristics of the curves.

In refining the model to be more conformable a study was made of some 49 curves for suitable pairs of  $\beta$  and  $\gamma$  (the points are shown as dots in Figure 2). From these curves the inflection point  $I$  and the tangent at the inflection point were calculated and  $BP$  taken to be the tangent there. Then

$$\sigma_{ip} = \text{length } OB + \text{length } BI \quad (16)$$

was calculated. The intercept  $c$  was given by a formula of Petersen (16) and  $a$  and  $b$  were determined from the tangent at the point of inflexion. The four quantities  $a, b, c, \sigma_{ip}$  were then represented as polynomials in  $\beta$  and  $\gamma$  suitably scaled

$$a = \sum_{i=1}^5 \sum_{j=1}^5 c_{ij}(a) (2\beta)^{i-1} (\gamma/25)^{j-1} \quad (17)$$

etc. Values of the coefficients  $c_{ij}(a)$ ,  $c_{ij}(b)$ ,  $c_{ij}(c)$ , and  $c_{ij}(\sigma_{ip})$  are given in Table 1. The search for the best coefficients, an optimization in 25 variables, took less than a minute of computer time on the CDC 6600. A secondary test of the fit is to determine the relationship between  $\beta$  and  $\gamma$  such that the tangent at the inflexion point is vertical ( $a = b$ ), since this is the condition for uniqueness. The agreement with the exact uniqueness condition is seen to be good as shown by the crosses in Figure 2.

Having determined  $\sigma_{ip}$ ,  $a$ ,  $b$ , and  $c$  independently of the shape of the corners, the representation of these was refined to make them less symmetrical. The corner shape parameters  $m$  and  $n$  were made functions of  $\sigma$  and the curve itself separated into two forms according as  $\sigma$  was greater or less than  $\sigma_{ip}$ . The formulae are thus

$$\sigma \leq \sigma_{ip} \begin{cases} X(\sigma) = V(\sigma; b, m(\sigma)) + \{(a-b)/l\} \\ \quad U(\sigma; b, m(\sigma)) \\ Z(\sigma) = \{(c-a)/l\} U(\sigma; b, m(\sigma)) \end{cases} \quad (18)$$

$$\sigma > \sigma_{ip} \begin{cases} X(\sigma) = b + \{(a-b)/l\} V(\sigma-b; l, n(\sigma)) \\ \quad + 2^{-1/2} U(\sigma-b; l, n(\sigma)) \\ Z(\sigma) = \{(c-a)/l\} V(\sigma-b; l, n(\sigma)) \\ \quad - 2^{-1/2} U(\sigma-b; l, n(\sigma)) \end{cases} \quad (19)$$

This has introduced a slight discontinuity at the point of inflection, but this will be small if  $m(\sigma)$  and  $n(\sigma)$  are large when  $\sigma = \sigma_{ip}$  and will be removed later.

The method of determining  $m(\sigma)$  and  $n(\sigma)$  was to consider chiefly those points that were far from the angle. Figure 4 shows the details for the first curve and those for the second are similar. The lines

$$(c-a)X(\sigma) + (l-a+b)Z(\sigma) \quad (20)$$

bear a constant value of  $\sigma$  in any such corner so that given any of the 36 points  $(X_{ci}, Z_{ci})$  the value  $\sigma$  can be quickly determined, as can also its distance from the broken line. But that distance uniquely defines a value of  $m$ , so that for each point near the corner a pair of values  $m_i, \sigma_i$  could be determined. A function  $m(\sigma)$  which interpolated these points would therefore be a perfect fit to them. All points a distance greater than 0.03 from the bent line were considered and for the first turn the best values of  $m_1$  and  $m_2$  were determined as functions of  $\beta$  and  $\gamma$  to give

$$m(\sigma) = m_1 + \frac{25 m_2}{1 + 25(\sigma_{ip} - \sigma)} \quad (21)$$

For the second term a little more fitting was required and  $n_1$  and  $n_2$  are used in the formula

$$n(\sigma) = n_1$$

$$+ \frac{100 n_2}{1 + 100(\sigma - \sigma_{ip})} + \frac{2}{25} H_1(\sigma - \sigma_{ip} - 2.5) \quad (22)$$

where  $H_1(x)$  is the integral of the Heaviside step function, zero for negative argument and  $H_1(x) = x$  for positive argument. As functions of  $\beta$  and  $\gamma$  the indices are given by the following formulae (as before  $c_{ij}(m_1)$ , etc. denote the coefficients in the polynomial giving  $m_1$ , etc.)

$$m_1 = \sum_{i=1}^5 \sum_{j=1}^5 c_{ij}(m_1) (2\beta)^{i-1} (\gamma/25)^{j-1} \quad (23)$$

$$m_2 = \max(\mu_2, 0.3),$$

$$\mu_2 = \sum_{i=1}^5 \sum_{j=1}^5 c_{ij}(\mu_2) (2\beta)^{i-1} (\gamma/25)^{j-1} \quad (24)$$

$$n_1 = \max(\nu_1, 0.5),$$

$$\nu_1 = \sum_{i=1}^6 \sum_{j=1}^6 c_{ij}(\nu_1) (2\beta)^{i-1} (\gamma/25)^{j-1} \quad (25)$$

$$n_2 = \max(\nu_2, N_2),$$

$$\nu_2 = \sum_{i=1}^5 \sum_{j=1}^5 c_{ij}(\nu_2) (2\beta)^{i-1} (\gamma/25)^{j-1} \quad (26)$$

$$N_2 = 0.05 + 0.4 (1.6 - \gamma/25)^2 \quad (27)$$

The values of the coefficients for  $m_1$ ,  $\mu_2$ ,  $\nu_1$ , and  $\nu_2$  are given in Table 2.

Since the above formulae are somewhat involved it will be useful to summarize their use in a series of steps which

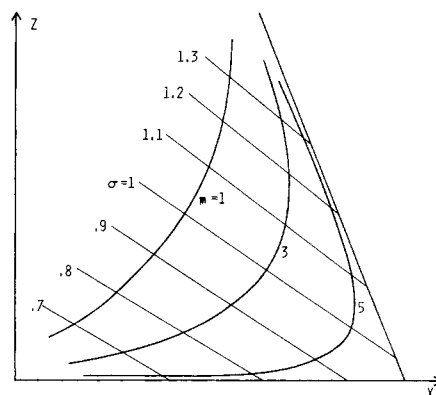


Fig. 4. The coordinate system in the first bend.

TABLE 1. INTERPOLATION COEFFICIENTS FOR  $a$ ,  $b$ ,  $c$  AND  $\sigma_{ip}$

$c_{ij}(a)$	1	2	3	4	5	$c_{ij}(b)$	1	2	3	4	5
1	+1.0359	-0.3204	-0.0425	+0.2023	-0.0815	1	-0.8502	+0.9662	-0.6261	+0.0151	+0.0759
2	-0.8254	-0.3062	-1.9323	+1.1788	-0.0840	2	+1.4208	-0.4654	+2.6977	-1.5614	+0.3556
3	+0.8243	-0.7610	+1.0342	-0.3757	-0.4382	3	+0.1042	-4.4825	+1.0312	-1.6338	+0.0089
4	-0.0172	-0.7595	+0.0371	+1.5592	-1.4153	4	-0.4870	+2.5573	+0.0560	+1.4105	+0.4375
5	+0.0176	+0.0308	-0.1770	+0.7573	-0.5404	5	-0.0028	+0.0345	-0.1351	-1.3406	+0.3415
$c_{ij}(c)$	1	2	3	4	5	$c_{ij}(\sigma_{ip})$	1	2	3	4	5
1	+0.4500	-0.0136	+0.1708	-0.2002	+0.0636	1	+0.3542	-0.8725	+0.4397	+0.0588	-0.0440
2	+0.1007	+0.5664	+0.5269	-0.1598	-0.0147	2	-0.7493	+2.0083	+0.1471	-0.3268	-0.0697
3	+0.0245	-0.1393	+0.3094	+0.1260	+0.1165	3	+0.2870	-0.4368	+0.4661	-0.6285	+0.5573
4	-0.0207	-0.0305	-0.0412	-0.0313	-0.2397	4	-0.0384	+0.0088	+0.0925	-0.6471	-0.1374
5	+0.0024	+0.0134	+0.0005	-0.0138	+0.0612	5	+0.0000	+0.0024	+0.0149	-0.0696	+0.3244

TABLE 2. INTERPOLATION COEFFICIENTS FOR  $m_1$ ,  $\mu_2$ ,  $\nu_1$ , AND  $\nu_2$ 

$c_{ij}(m_1)$	1	2	3	4	5	6	$c_{ij}(\mu_2)$	1	2	3	4	5
1	+0.9596	-1.9890	+3.8670	-8.2980	+3.9842		1	+3.1716	+3.6278	-2.1904	+4.0468	-2.2326
2	+14.7166	-7.0062	+25.1898	+6.5480	-6.3926		2	-9.6130	+1.7016	-14.9610	-9.0660	+5.7796
3	-8.9400	-11.3426	-15.4648	-16.9270	-3.2488		3	+9.9852	+1.9244	+8.7872	+14.6204	+4.6210
4	+0.9046	+9.9382	+13.6384	-10.2224	+22.3106		4	-1.6484	-9.9504	-3.1666	+12.0402	-22.7840
5	-0.0384	-1.5164	-0.6604	-1.7530	-4.3546		5	+0.0000	+2.8420	-3.5130	+4.1906	+2.1884

$c_{ij}(\nu_1)$	1	2	3	4	5	6	$c_{ij}(\nu_2)$	1	2	3	4	5
1	+3.7192	+2.7312	-8.0225	+5.0150	-1.0421	-0.0160	1	+2.9114	-4.7415	+4.3337	-0.9649	-0.0540
2	-6.5638	+2.8117	-2.0460	+5.0919	-0.2956	+0.0140	2	+0.4908	-6.2146	+7.8233	-4.5376	+0.2506
3	+3.2435	+5.2609	-2.8072	-2.3682	-5.4979	+0.0120	3	+0.5070	-0.4729	+5.6429	-5.8145	+1.3126
4	-0.4765	-2.6363	-1.8945	+1.4418	+6.7477	+0.0740	4	+0.0028	-0.3720	-1.1434	+1.4972	+1.8528
5	+0.0000	+0.0540	+1.7000	-0.7316	-2.5099	-0.0400	5	-0.0846	+0.1096	+0.5886	-1.3756	-1.9932
6	+0.0000	+0.0000	+0.0140	-0.0140	-0.0260	-0.0480						

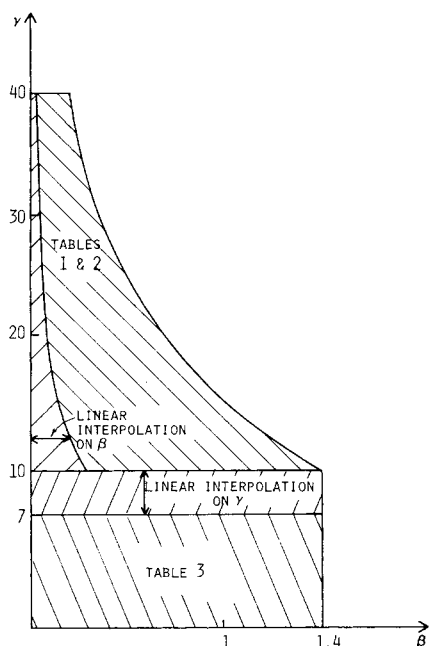


Fig. 5. Regions of validity of the several parts of the program.

may be followed in accordance with the following directions.

1. Given values of  $\beta$  and  $\gamma$ , first determine the region of Figure 5 within which  $(\beta, \gamma)$  lies.
  - a. If  $10 \leq \gamma \leq 40$ ,  $1.5 \leq \beta \leq 14$ , proceed to Step 2
  - b. If  $10 \leq \gamma \leq 40$ ,  $\beta < 1.5$ , proceed to Step 5
  - c. If  $0 \leq \beta \leq 1.4$ ,  $7 < \gamma < 10$ , proceed to Step 8
  - d. If  $0 \leq \beta \leq 1.4$ ,  $0 \leq \gamma < 7$ , proceed to Step 6
  - e. If none of these, the interpolation routine cannot be used.
2. Determine the parameters  $a$ ,  $b$ ,  $c$ , and  $\sigma_{ip}$  from Equation (17) and Table 1. Proceed to Step 3.
3. Determine the parameters  $m_1$ ,  $m_2$ ,  $n_1$ ,  $n_2$  from Equations (23) to (26) and Table 2. Proceed to Step 4.
4. Determine  $X(\sigma)$ ,  $Z(\sigma)$  from Equations (18), (19), (21), and (22). The functions  $U$  and  $V$  are defined by Equations (9) and (10).
5. Determine  $\beta' = 1.5/\gamma$ . Perform Steps 2 and 3 for the point  $(\beta', \gamma)$ . Interpolate linearly in  $\beta$  between the values of  $a$ ,  $b$ ,  $c$ ,  $\sigma_{ip}$ ,  $m_1$ ,  $m_2$ ,  $n_1$ ,  $n_2$  so found and those given in Equation (29). (Cf. remarks immediately following this equation.) Proceed to Step 4.
6. Determine  $a$ ,  $b$ ,  $c$ ,  $\sigma_{ip}$  from Equation (30) and Table

3. Proceed to Step 7.

7. Determine  $m_1$ ,  $m_2$ ,  $n_1$ ,  $n_2$  for the point  $(\beta, 10)$  by Step 2 and interpolate linearly on  $\gamma$  between these values and those given for  $\gamma = 0$  in Equation (29). Proceed to Step 4.

8. Determine  $a$ ,  $b$ ,  $c$ , and  $\sigma_{ip}$  for  $(\beta, 10)$  by Step 2 and for  $(\beta, 7)$  by Step 6. Interpolate linearly on  $\gamma$ . Proceed to Step 7.

#### Extension to $\beta\gamma < 1.5$ , $\gamma < 10$

If  $\beta\gamma < 1.5$  the broken line cannot be determined for there is no inflection point. When  $\beta\gamma = 0$  the isothermal effectiveness factor

$$\eta = 3 \{ \phi \coth \phi - 1 \} / \phi^2 \quad (28)$$

obtains. This may be fitted quite well by the set of parameter values

$$a_0 = 0.635, \quad b_0 = -0.1, \quad c_0 = 0.4771, \quad \sigma_{ip0} = 0.1 \quad (29)$$

$$m_{10} = 3, \quad m_{20} = 1, \quad n_{10} = 1.8, \quad n_{20} = 1.45$$

The extension into the region  $\beta\gamma \leq 1.5$ ,  $10 \leq \gamma \leq 40$  is made by linear interpolation between these values and the values for  $a$ ,  $b$ ,  $\dots$ ,  $n_2$  obtained for  $\gamma' = \gamma$  and  $\beta' = 1.5/\gamma$ . Thus for example given  $a(\beta, \gamma)$  in this region  $a'$ ,  $b'$ ,  $\dots$ ,  $n_2'$  are calculated from Tables 1 and 2 for  $\beta' = 1.5/\gamma$ ,  $\gamma' = \gamma$  and then  $a = a_0 + (a' - a_0)(\beta/\beta')$  etc.

The region  $0 \leq \gamma \leq 7$ ,  $0 \leq \beta < 1.4$  can be handled by by interpolation formulae of the form

$$a = a_0 + \sum_{i=1}^3 \sum_{k=1}^2 d_{ik}(a) (2\beta)^i (\gamma/25)^k \quad (30)$$

etc. where the coefficients  $d_{ik}$  are given in Table 3 for  $a$ ,  $b$ ,  $c$ , and  $\sigma_{ip}$ . Values of these parameters between  $\gamma = 7$  and  $\gamma = 10$  are obtained by linear interpolation on  $\gamma$ . Values of  $m_1$ ,  $m_2$ ,  $n_1$ , and  $n_2$  can be interpolated linearly over the whole range from  $\gamma = 0$  to  $\gamma = 10$ .

Two final refinements may be made. If  $\sigma < -2$  it is sufficiently accurate to set

$$X(\sigma) = X(-2) + \sigma + 2, \quad Z(\sigma) = Z(-2) \quad (31)$$

On the other hand if  $\sigma > 20$

$$X(\sigma) = X(20) + 2^{-1/2} (\sigma - 20),$$

$$Z(\sigma) = Z(20) - 2^{-1/2} (\sigma - 20) \quad (32)$$

Also the continuity at the inflection point

$$\sigma = \sigma_{ip}, \quad X_{ip} = b + \{ (a - b)/l \} (\sigma_{ip} - b),$$

$$Z_{ip} = \{(c - a)/l\} (\sigma_{ip} - b) \quad (33)$$

can be ensured by linear interpolation between  $(X(\sigma_{ip} - 0.05), Z(\sigma_{ip} - 0.05))$  and  $(X_{ip}, Z_{ip})$  and between  $(X_{ip}, Z_{ip})$  and  $(X(\sigma_{ip} + 0.05), Z(\sigma_{ip} + 0.05))$ .

### The Computer Program and its Accuracy

The last three paragraphs with Tables 1, 2, and 3 give full detail of the interpolation formulae. The combined effect sounds complicated, but computation is extremely rapid. A flow chart and computer program in Fortran IV are given in the thesis of J. G. Jouven obtainable from University Microfilms.

To illustrate the accuracy, a typical curve from region 1 and the worst curve of that region are shown in Figure 6. Full details of the variance of the fit to each curve can be found in the thesis. The two shaded regions in Figure 2 are of better than 5% and 10% accuracy respectively.

The determination of  $\eta$  by the integration of Equations (1), (2), and (3) can be done about 20 times a second on the CDC 6600. The recovery of the value of  $\eta$  from our routine can be done 1,100 times a second so that it is about 55 times faster than direct integration.

### Applications of the Parametric Representation

The most obvious application of the representation of the effectiveness factor is in the step-by-step calculation of the packed bed. This has been done by Liu (12) and will not be pursued here. As Liu remarks, when there is more than one steady state the full transient equations must be solved if one is to know which steady state is approached. The only ones that can be ruled out are the unstable steady states corresponding as Amundson and Raymond (1) have shown to the part of the  $\eta$ ,  $\varphi$ -curve that lies between the two vertical tangents. One of the uses of this program is to find these points of vertical tangency and this can be done very rapidly. Stewart and Villadsen (17) have given a rapid graphical method by which this can be done with reasonable accuracy. The only comment that may be made on fixed bed calculations is to note that in many cases the time constant in the particle is much shorter than that of the reactor as a whole and that a pseudo-steady state approximation may be quite valid for the particle under all but the most violent transitions. It may also be reasonable to assert a proximate-steady state hypothesis and claim that when in a step-by-step calculation a region of nonuniqueness is reached that the nearest stable steady state should be chosen. Questions of this sort have been considered elsewhere (3 to 5).

The application that will be treated in more detail is the use that may be made of the program to obtain the effectiveness factor when external resistances to heat and mass transfer are considered. The parameters  $\phi$ ,  $\beta$ , and  $\gamma$  are based on  $T_s$  and  $c_s$  the surface concentration and tem-

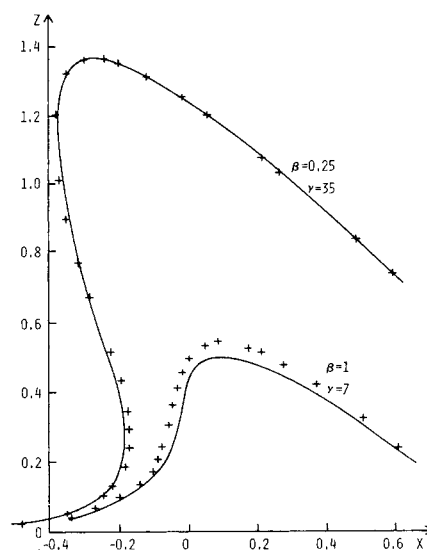


Fig. 6. Illustrating the accuracy of the representation. The curve  $\beta = 0.25$ ,  $\gamma = 35$  is typical: that for  $\beta = 1$ ,  $\gamma = 7$  is the worst fit in region 1.

perature, and  $\eta$  is a function of them. If a suffix  $f$  denotes the values of  $c$  and  $T$  in the fluid far from the particle or parameter values based on them, then

$$\begin{aligned} \beta_f &= (-\Delta H) D_e c_f / k_e T_f = (c_f T_s / c_s T_f) \beta \\ \gamma_f &= E / R_g T_f = (T_s / T_f) \gamma \\ \phi_f^2 &= R^2 \rho_b S_g k(T_f) / D_e = \phi^2 e^{\gamma_f - \gamma} \\ \eta_f &= \frac{\text{total reaction rate in sphere}}{\text{total reaction rate at } c_f, T_f} \\ &= \frac{\eta(4/3) \pi R^3 \rho_b S_g c_s k(T_s)}{(4/3) \pi R^3 \rho_b S_g c_f k(T_f)} = \eta \frac{c_s}{c_f} e^{\gamma_f - \gamma} \end{aligned} \quad (34)$$

But the surface concentrations  $c_s$  and  $T_s$  are related to  $c_f$  and  $T_f$  by the heat and mass balances over the particle as a whole, namely

$$4\pi R^2 h(T_s - T_f) = (-\Delta H) \frac{4}{3} \pi R^3 \rho_b S_g \eta c_s k(T_s) \quad (35)$$

and

$$4\pi R^2 k_c(c_f - c_s) = \frac{4}{3} \pi R^3 \rho_b S_g \eta c_s k(T_s) \quad (36)$$

where  $h$  and  $k_c$  are the transfer coefficients for heat and mass. Defining Nusselt and Sherwood numbers by

$$Nu = 2Rh/k_e, \quad Sh = 2Rk_c/D_e \quad (37)$$

gives the equations

$$Sh \left(1 - \frac{c_s}{c_f}\right) = \frac{2}{3} \frac{c_s}{c_f} \eta \phi^2 = \frac{2}{3} \eta_f \phi_f^2 \quad (38)$$

$$Nu \left(\frac{T_s}{T_f} - 1\right) = \beta_f \frac{2}{3} \frac{c_s}{c_f} \eta \phi^2 = \beta_f \frac{2}{3} \eta_f \phi_f^2 \quad (39)$$

The problem then is to find all the solutions of these equations given  $\phi_f$ ,  $\beta_f$ ,  $\gamma_f$ ,  $Nu$ , and  $Sh$ . This is accomplished by assuming a value for  $T_f/T_s = \tau$  in the range (0, 1). Then

$$\frac{c_s}{c_f} = 1 - \frac{Nu}{\beta_f Sh} \frac{1 - \tau}{\tau}, \quad \beta = \frac{c_s}{c_f} \tau \beta_f, \quad \gamma = \tau \gamma_f \quad (40)$$

TABLE 3. INTERPOLATION COEFFICIENTS FOR  $a$ ,  $b$ ,  $c$ , AND  $\sigma_{ip}$

		$k$				$k$	
		1	2			1	2
$i$	$d_{ik}(a)$			$d_{ik}(b)$			
	1	-0.3562	-1.2130	-1.5692	+3.7114		
	2	-0.2238	-0.4576	+0.5100	+0.1892		
	3	+0.0480	+0.1604	-0.0680	-0.2566		
$i$	$d_{ik}(c)$			$d_{ik}(\sigma_{ip})$			
	1	+0.8076	+0.5286	+0.2720	+0.5752		
	2	-0.0886	-0.0026	-0.1954	+0.1948		
	3	0	-0.0054	+0.0126	+0.0168		

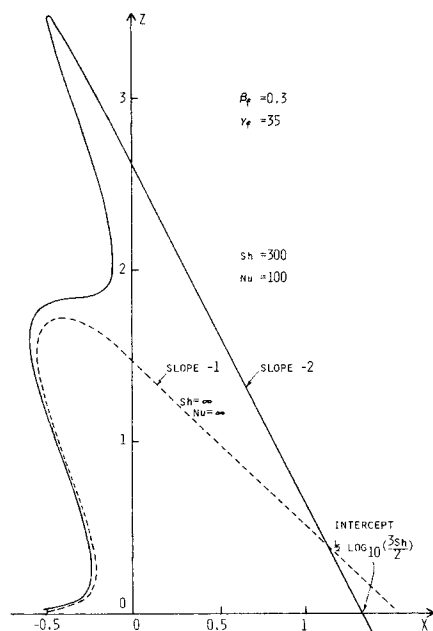


Fig. 7. The effectiveness factor with external mass and heat transfer resistances.

can be calculated. Moreover  $\eta\phi^2$  can be calculated in terms of  $\tau$  from the logarithmic relation

$$Y = \log_{10} \eta\phi^2 = \log_{10} \left[ \frac{3}{2} Sh \left( \frac{c_f}{c_s} - 1 \right) \right] \quad (41)$$

But  $Y$  is a monotonic function of  $\sigma$  so that the value of  $\sigma(\tau)$  can be obtained and it suffices to find all the values of  $\sigma$  that satisfy  $\phi_f^2 = \phi^2 \exp(\gamma - \gamma_f)$ , that is

$$X(\sigma) = \log_{10} \phi_f + 0.2171 (1 - \tau) \gamma_f \quad (42)$$

Finally  $\eta_f$  is given by  $\eta_f = c_s \eta \phi^2 / c_f \phi_f^2$ . There are at most five solutions of this last equation. A plot of  $\eta_f$  versus  $\phi_f$  for  $\beta_f = 0.3$ ,  $\gamma_f = 35$ ,  $Sh = 300$ ,  $Nu = 100$  is shown in Figure 7.

The determination of  $\eta_f$  can of course be incorporated in the step-by-step calculation down the fixed bed. The time saved by our parametric representation is considerable and a fixed bed of 150 steps can be done on the CDC 6600 in a little less than 10 sec. The individual values of  $\eta_f$  using the Robin boundary conditions (35) and (36) can be obtained in about 0.03 sec.

#### ACKNOWLEDGMENT

We are indebted to the National Science Foundation for the support of a study of chemical reactor behavior, of which this forms a part. (Grant GK1367). The address of University Microfilms is Ann Arbor, Michigan 48104.

#### NOTATION

$a, b, c$  = parameters of the broken line  
 $c_{ij}(\cdot)$  = coefficients in interpolation formulae  
 $c(r)$  = concentration at radius  $r$   
 $c_f, c_s$  = concentration in bulk fluid and on surface  
 $D_e$  = effective diffusivity of reactant  
 $d_{ik}(\cdot)$  = coefficients in interpolation, Equation (30)  
 $E$  = activation energy  
 $F$  = function defined by Equation (8)

$h$  = heat transfer coefficient  
 $k_c$  = mass transfer coefficient  
 $k_e$  = effective thermal conductivity of pellet  
 $k(T)$  = first-order rate constant per unit catalytic area  
 $l$  = parameter of the broken line  
 $m, n$  = corner parameters  
 $Nu$  = Nusselt number  
 $R$  = radius of spherical pellet  
 $R_g$  = gas constant  
 $Sh$  = Sherwood number  
 $S_g$  = catalytic area per gram  
 $U, V, W$  = functions defined by Equations (9), (10), and (11)  
 $x$  = dimensionless concentration,  $c(r)/c_s$   
 $X$  =  $\log_{10} \phi$   
 $Y$  =  $2X + Z$   
 $Z$  =  $\log_{10} \eta$   
 $\beta$  = Prater temperature,  $(-\Delta H) D_e c_s / k_e T_s$   
 $\gamma$  =  $E / RT_s$   
 $\delta$  =  $\beta \gamma$   
 $\Delta H$  = heat of reaction  
 $\eta$  = effectiveness factor  
 $\rho$  = dimensionless radius,  $r/R$   
 $\rho_b$  = bulk density of catalyst pellet  
 $\sigma$  = parameter along  $\eta, \phi$ -curve  
 $\tau$  =  $T_f / T_s$   
 $\phi$  = Thiele modulus  $R \{ \rho_b S_g k(T_s) / D_e \}^{1/2}$

#### Subscripts

$c_i$  =  $i$ th calculated point  
 $f$  = based on bulk fluid conditions  
 $ip$  = inflection point  
 $s$  = based on surface conditions

#### LITERATURE CITED

- Amundson, N. R., and L. Raymond, *Can. J. Chem. Eng.*, **42**, 173 (1964).
- Amundson, N. R., and R. E. Schilson, *Chem. Eng. Sci.*, **13**, 237 (1961).
- Aris, R., Proc. 1st Int. Symp. on Chem. Reaction Eng., Washington, D. C., June 1970, ACS Publications, Washington, D. C., 1971 p.
- Aris, R., *Chem. Eng. J.*, **2**, 140 (1971).
- , and D. Schruben, *ibid.*, 179.
- Carberry, J. J., *AIChE J.*, **7**, 350 (1961).
- , *Chem. Eng. Sci.*, **17**, 675 (1962).
- , *Ind. Eng. Chem.*, **58**, 40 (Oct. 1966).
- Cunningham, R. A., J. J. Carberry, and J. M. Smith, *AIChE J.*, **11**, 637 (1965).
- Damkohler, G., *Z. Phys. Chem.*, **A193**, 16 (1943).
- Juttner, F., *Zeit. Phys. Chem.*, **65**, 595 (1909).
- Liu, Shean-Lin, *AIChE J.*, **16**, 742 (1970).
- McGreavy, C., and D. Cresswell, *Can. J. Chem. Eng.*, **47**, 583 (1969).
- Mercer, M. C., and Rutherford Aris, submitted to *Latin Am. J. Chem. Eng.*
- Metzner, A. B., and J. D. Tinkler, *Ind. Eng. Chem.*, **53**, 663 (1961).
- Petersen, E. E., "Chemical Reaction Analysis," Prentice-Hall, Englewood Cliffs, N. J. (1965).
- Stewart, W. E., and Jon Villadsen, *AIChE J.*, **15**, 28 (1969).
- Thiele, E. W., *Ind. Eng. Chem.*, **31**, 916 (1939).
- Weisz, P. B., and J. S. Hicks, *Chem. Eng. Sci.*, **17**, 265 (1962).
- Wilde, D., "Optimum Seeking Methods," Prentice-Hall, Englewood Cliffs, N. J. (1964).
- Zeldovich, Ya. B., *Acta Physicochim. URSS*, **10**, 583 (1939).

Manuscript received July 28, 1971; paper accepted November 2, 1971.